*Medicine*

*Oncology fields*

Okayama University *Year* 2004

# Visualization of intrathoracically disseminated solid tumors in mice with optical imaging by telomerase-specific amplification of a transferred green fluorescent protein gene

Tatsuo Umeoka, *Okayama University*
Takeshi Kawashima, *Okayama University*
Shunsuke Kagawa, *Okayama University*
Fuminori Teraishi, *Okayama University*
Masaki Taki, *Okayama University*
Masahiko Nishizaki, *Okayama University*
Satoru Kyo, *Okayama University*
Katsuyuki Nagai, *Okayama University*
Yasuo Urata, *Okayama University*
Noriaki Tanaka, *Okayama University*
Toshiyoshi Fujiwara, *Okayama University*

# Visualization of Intrathoracically Disseminated Solid Tumors in Mice with Optical Imaging by Telomerase-specific Amplification of a Transferred Green Fluorescent Protein Gene[1]

Tatsuo Umeoka, Takeshi Kawashima, Shunsuke Kagawa, Fuminori Teraishi, Masaki, Taki, Satoru Kyo, Katsuyuki Nagai, Yasuo Urata, Noriaki Tanaka, and Toshiyoshi Fujiwara[2]

Division of Surgical Oncology, Department of Surgery, Okayama University Graduate School of Medicine and Dentistry, Okayama 700-8558, Japan [T. U., T. K., S. K., F. T., M. T., N. T., T. F.];

Center for Gene and Cell Therapy, Okayama University Hospital, Okayama 700-8558, Japan[S. K., T. F.]

Department of Obstetrics and Gynecology, Kanazawa University School of Medicine, Kanazawa 920-8641, Japan[S. K.]

Oncolys BioPharma, Inc., Tokyo 106-0031, Japan [K. N., Y. U].

**Running title:** VISUALIZATION OF TUMORS BY GFP AMPLIFICATION

**Key words:** GFP; adenovirus; telomerase; replication; gene therapy.

**Footnotes:**

[1]This work was supported in part by grants from the Ministry of Education, Science, and Culture, Japan; and by grants from the Ministry of Health and Welfare, Japan.

[2] To whom all correspondence and requests for reprints should be addressed at, Center for Gene and Cell Therapy, Okayama University Hospital, 2-5-1 Shikata-cho, Okayama 700-8558, Japan. E-mail: toshi_f@md.okayama-u.ac.jp

[3]The abbreviations used are: CCD, cooled charged-coupled device; GFP, green fluorescent protein; hTERT, human telomerase reverse transcriptase; HUVEC, human umbilical endothelial cells; IRES, internal ribosome entry site; MOI, multiplicity of infection; NHLF, normal human lung fibroblasts; PFU, plaque-forming units.

## ABSTRACT

Currently available methods for detection of tumors *in vivo* such as X-ray, computed tomography, and ultrasonography are noninvasive and well studied; the images, however, are not specific for tumors. Direct optical imaging of tumor cells *in vivo* that can clearly distinguish them from surrounding normal tissues may be clinically useful. Here, we describe a new approach to visualizing tumors whose fluorescence can be detected using tumor-specific replication-competent adenovirus (OBP-301, "Telomelysin") in combination with replication-deficient adenovirus expressing GFP (Ad-*GFP*). Human telomerase reverse transcriptase (hTERT) is the catalytic subunit of telomerase, which is highly active in cancer cells, but is quiescent in most normal somatic cells. We constructed an adenovirus 5 vector, in which the hTERT promoter element drives expression of *E1A* and *E1B* genes linked with an IRES, and showed that OBP-301 replicated efficiently exclusively in human cancer cells, but not in normal cells such as human fibroblasts. When the human lung and colon cancer cell lines H1299 and SW620 were infected with Ad-*GFP* at low multiplicity of infection (MOI), GFP expression could not be detected under a fluorescence microscope; in the presence of OBP-301, however, Ad-*GFP* replicated in these tumor cells and showed strong green signals. In contrast, co-infection of OBP-301 and Ad-*GFP* did not show any signals in normal cells such as WI-38 fibroblasts. We also found that established subcutaneous tumors could be visualized following intratumoral injection of OBP-301 and Ad-*GFP*. A549 human lung tumors and SW620 human colon tumors transplanted into BALB/c *nu/nu* mice were intratumorally injected with $8 \times 10^5$ plaque forming units

(PFU) of Ad-*GFP* in combination with 8 x $10^6$ PFU of OBP-301. Within 3 days of treatment, the fluorescence of the expressed GFP became visible by 3CCD camera in these tumors, whereas intratumoral injection of Ad-*GFP* alone could not induce GFP fluorescence. Moreover, intrathoracic administration of Ad-*GFP* and OBP-301 could visualize disseminated A549 tumor nodules in mice following intrathoracic implantation. Our results indicate that intratumoral or intrathoracic injection of Ad-*GFP* in combination with OBP-301 might be a useful diagnostic method that provides a foundation for future clinical application.

## INTRODUCTION

A variety of imaging technologies is being investigated as tools for cancer diagnosis, detection, and treatment monitoring. Improvements in methods of external imaging such as computed tomography (CT), magnetic resonance imaging (MRI), and ultrasound techniques have increased the sensitivity for visualizing tumors and metastases (1, 2); a limiting factor in structural and anatomical imaging, however, is the inability to specifically identify malignant tissues. Histopathological examination is still the most effective method for the detection of neoplastic lesions. Thus, tumor-specific imaging would be of considerable value in treatment of human cancer by defining the location and area of tumors without microscopic analysis. In particular, if tumors too small for direct visual detection and therefore not detectable by direct inspection could be imaged *in situ*, surgeons could precisely excise tumors with appropriate surgical margins. This paradigm requires an appropriate "marker" that can facilitate visualization of physiological or molecular events that occur in tumor cells but not normal cells.

Molecular and functional monitoring of cellular processes has become a reality with the development of the green fluorescent protein (GFP)[3] technology, which was originally identified from the jellyfish *Aequorea Victoria* (3-5). GFP is able to specifically label biological molecules and cellular structures, and can be sensitively detected by a variety of optical techniques. These labels can be detected in living tissues because of the relatively non-invasive nature of fluorescence, thus allowing transient and dynamic events to be visualized and measured (6-10). In addition, as GFP is

genetically encoded, cells can be labeled by introducing the exogenous *GFP* gene. Indeed, Yang *et al.* have shown that GFP-expressing tumors growing and metastasizing in intact animals could be viewed externally with a whole-body optical imaging system (11). Moreover, transgene expression could be also monitored by utilizing an adenovirus vector expressing the *GFP* gene. These observations indicate that the GFP-based approach might be feasible as well as practical for real-time tumor imaging in living mammalians.

To specifically distinguish tumors from normal tissues, an appropriate strategy to make tumor cells selectively fluorescent is required. We previously constructed the tumor-specific replication-selective adenovirus (OBP-301, "Telomelysin"), in which the human telomerase reverse transcriptase (hTERT) promoter element drives expression of *E1A* and *E1B* genes linked with an internal ribosome entry site (IRES), and demonstrated the selective replication and the antitumor effect in human cancer cells *in vitro* and *in vivo* (12). As more than 85% of human cancer cells, but not most somatic normal cells, display telomerase activity (13, 14), we hypothesized that OBP-301 infection could complement *E1* gene functions and facilitate replication of E1-deleted replication-deficient vectors selectively in tumor cells when co-infected.

In the present study, using a replication-deficient adenovirus expressing the GFP gene in combination with OBP-301, we demonstrate a real-time fluorescence optical imaging of pleural dissemination of human non-small cell lung cancer cells in an orthotopic murine model. This novel molecular imaging technique could be feasible for *in vivo* detection of disseminated small tumor nodules.

## MATERIALS AND METHODS

**Cells and Culture Conditions.** The human non-small cell lung cancer cell lines H1299, H358, and H226Br and the human colorectal carcinoma cell lines SW620, LoVo, and DLD-1 were routinely propagated in monolayer culture in RPMI 1640 medium supplemented with 10% FCS. The human non-small cell lung cancer cell line A549 was cultured in Dulbecco's Modified Eagle Medium (DMEM) containing Nutrient Mixture (Ham's F12). The transformed embryonic kidney cell line 293 was grown in DMEM containing high glucose (4.5 g/l) and supplemented with 10% FCS. The normal human lung diploid fibroblast cell line WI38 (JCRB0518) was obtained from the Health Science Research Resources Bank (HSRRB, Japan), and grown in Eagle's minimal essential medium with 10% FCS. The normal human lung fibroblast cell line NHLF was purchased from TaKaRa Biomedicals (Kyoto, Japan) and cultured in the medium recommended by the manufacturer. The human umbilical vascular endothelial cell line HUVEC was kindly provide by Dr. Masayoshi Namba (Okayama University, Okayama, Japan) and propagated in monolayer culture in CSC certified medium with 100 units/ml penicillin and 100 mg/ml streptomycin.

**Recombinant Adenoviruses.** The recombinant replication-selective, tumor-specific adenovirus vector was previously constructed and characterized (12). The resultant virus was named OBP-301 ("Telomelysin"). The adenoviral vector containing GFP cDNA (Ad-*GFP*) was also used. Viral stocks were quantified by a plaque-forming assay using 293 cells and stored at -80$^{o}$C.

**Quantitative Real-time PCR Analysis.** Total RNA from the tumor samples

and cultured cells was obtained using the RNeasy Mini Kit (Qiagen, Chatsworth, CA). Approximately 0.1 μg of total RNA was used for reverse transcription. Reverse transcription was performed at 22°C for 10 min and then at 42°C for 20 min. The *hTERT* mRNA copy number was determined by real-time quantitative RT-PCR using a LightCycler instrument and a LightCycler DNA TeloTAGGG Kit (Roche Molecular Biochemicals, Indianapolis, IN). PCR amplification began with a 60-sec denaturation step at 95°C and then 40 cycles of denaturation at 95°C for 15 sec, annealing at 58°C for 10 sec, and extension at 72°C for 9 sec.

**Fluorescent Microscopy.** Human cancer cell lines (SW620, A549, and H1299) and normal cells (WI-38, NHLF, and HUVEC) were infected with either 0.1 multiplicity of infection (MOI) of Ad-*GFP* alone or in combination with 1 MOI of OBP-301 *in vitro*. Expression of the *GFP* gene was assessed and photographed (× 200 magnification) by an Eclipse TS-100 fluorescent microscope (Nikon, Tokyo, Japan) 24 hours after infection.

**Animal Experiments.** The experimental protocol was approved by the Ethics Review Committee for Animal Experimentation of our institution. SW620 and A549 xenografts were produced on the back in 5-week-old female BALB/c *nu/nu* mice by subcutaneous injection of $5 \times 10^6$ SW620 or A549 cells in 500 μl of Hank's balanced salt solution (HBSS). Three weeks after tumor cell inoculation, both tumors were intratumorally injected with either Ad-*GFP* ($8 \times 10^5$ PFU/50 μl) alone or Ad-*GFP* ($8 \times 10^5$ PFU/25 μl) plus OBP-301 ($8 \times 10^6$ PFU/25 μl). Mice were anesthetized by intraperitoneal injection of pentobarbital (50 mg/kg) on days 1, 2, 3, 7, and 14 after virus injection, and examined for GFP expression. As the control, viruses were

subcutaneously injected into non-tumor-bearing mice. To generate an orthotopic model of pleural dissemination, female BALB/c *nu*/*nu* mice were intrathoracically injected with cell suspension of A549 cells at a density of $5 \times 10^6$ cells/200 μl through a 27-gauge needle. Two weeks later, $4 \times 10^7$ PFU/50 μl of Ad-*GFP* and $4 \times 10^7$ PFU/50 μl of OBP-301 were injected into the thoracic space by the same technique. Five days after virus injection, mice were sacrificed and their thoracic spaces were examined.

**Cooled Charged-coupled Device (CCD) Imaging.** *In vivo* GFP fluorescence imaging was acquired by illuminating the animal with a Xenon 150 W lamp. The re-emitted fluorescence was collected through a long pass filter on a Hamamatsu C5810 3-chip color CCD camera (Hamamatsu Photonics Systems, Hamamatsu, Japan). High-resolution image acquisition was accomplished using an EPSON PC. Images were processed for contrast and brightness with the use of Adobe Photoshop 4.0.1J software.

## RESULTS

**hTERT Levels in Human Cancer and Normal Cells.** Telomerase is a novel marker for malignant diseases (15). To confirm the specificity of telomerase activity in human cancer cells, expression of hTERT mRNA, which plays a key role in telomerase activation (16), was measured in a panel of human tumor and normal cell lines using a real-time RT-PCR method. All tumor cell lines, including human non-small cell lung cancer A549, H226Br, and H1299 cell lines and human colorectal cancer SW620, LoVo, and DLD-1 cell lines, expressed detectable levels of *hTERT* mRNA, although the levels of expression varied widely (Fig. 1A). In contrast, human fibroblast cells such as WI38 and NHLF were negative for hTERT expression. HUVEC transformed with the SV40 large T-antigen gene also exhibited no hTERT mRNA expression. 293 cells are known to be telomerase-positive and were used as a positive control. These results suggest that the hTERT promoter element can be used to target human cancer.

**Selective Visualization of Human Cancer Cells *In Vitro*.** To selectively enhance GFP transgene expression in human cancer cells, we used a tumor- or telomerase-specific replication-selective adenovirus, OBP-301, and a replication-deficient Ad-*GFP*. Schematic DNA structures of OBP-301 and Ad-*GFP* are shown in Fig. 1B. SW620, A549, and H1299 human cancer cells expressed bright GFP fluorescence as early as 24 hours after co-infection of Ad-*GFP* (0.1 MOI) and OBP-301 (1.0 MOI) (Fig. 2). The fluorescence intensity gradually increased until approximately 3 days after infection followed by rapid cell death due to the cytopathic effect of OBP-301 (data not shown). Ad-*GFP* infection alone at an MOI of 0.1 caused neither

GFP expression nor cytotoxicity in SW620 and A549 cells. Only a faint fluorescence could be detected in H1299 cells by 0.1 MOI of Ad-*GFP* infection, because H1299 cells are highly sensitive to adenovirus infection. In contrast, normal human cells, including WI-38, NHLF, and HUVEC, were completely negative for GFP expression after co-infection with Ad-*GFP* and OBP-301. These results indicate that Ad-*GFP* can replicate exclusively in human cancer cells in the presence of OBP-301, leading to tumor cell-specific GFP fluorescence expression *in vitro*.

**Dose-dependent Intensity of Fluorescence by Ad-*GFP* Injection into Mice.** To selectively detect tumor tissues *in vivo*, non-specific *GFP* transgene expression in normal organs must be avoided. We first determined the optimal dose of Ad-*GFP* that could not induce detectable GFP fluorescence in normal tissues. Non-tumor-bearing mice were subcutaneously injected with increasing doses of Ad-*GFP* alone and then monitored for fluorescence intensity over time with the CCD non-invasive imaging system. As shown in Fig. 3, mice administered $1.3 \times 10^9$ and $1.3 \times 10^8$ PFU of Ad-*GFP* displayed high and moderate GFP fluorescence signals in the skin, respectively, within 24 hours post-injection. In contrast, the *GFP* transgene expression was not visible over a 7-day period after injection of $1.3 \times 10^7$ or $1.3 \times 10^6$ PFU of Ad-*GFP*. Thus, $10^8$ PFU was considered the lowest dose of Ad-*GFP* that induces non-specific GFP signals in normal tissues.

**Selective Visualization of Subcutaneously Growing Human Tumors *In Vivo*.** To further confirm the specificity of the GFP-based fluorescent optical detection of tumors *in vivo*, we performed a set of control experiments. In the control group of non-tumor-bearing animals that received subcutaneous injection with $8 \times 10^5$ PFU of

Ad-*GFP* plus $8 \times 10^6$ PFU of OBP-301, no apparent GFP signals were detected in the skin over 7 consecutive days (Fig. 4A). Moreover, injection of Ad-*GFP* at the density of $8 \times 10^5$ PFU alone into subcutaneously established SW620 tumors resulted in no GFP fluorescence expression for at least 7 days post-injection (Fig. 4B).

We next examined the kinetics of *GFP* transgene expression in SW620 and A549 tumors after intratumoral injection of $8 \times 10^5$ PFU of Ad-*GFP* and $8 \times 10^6$ PFU of OBP-301. Treated mice displayed detectable intratumoral signals within 24 hours after local delivery of viruses (Fig. 5). Whole-body images of mice showed light spots in the tumor area, although complete tumor images were not observed. The fluorescence intensity reached maximum levels 3 to 7 days post-injection, and gradually decreased to the background fluorescence by 14 days after treatment. When mice were sacrificed 7 days after intratumoral injection of viruses, GFP expression was confined to the tumor; no GFP fluorescence was detected in various normal organs such as liver, kidney, spleen, small intestine, brain, heart, pancreas, ovary, and adrenal gland (data not shown).

**Selective Visualization of Pleural Dissemination of Human Lung Cancer Cells *In Vivo*.** We also evaluated the potential of GFP-based visualization of A549 human non-small cell lung cancer cells growing intrathoracically in athymic *nu*/*nu* mice. We previously reported that, when A549 cells were inoculated into the thoracic space, dissemination of tumors appeared in all mice 14 days after tumor injection (17). As shown in Fig. 6, the optical CCD imaging of the thoracic cavity following a midsternal thoracotomy demonstrated that disseminated tumor nodules in the visceral pleura, parietal pleura, diaphragmatic pleura and mediastinum could be detected as light

emitting spots by intrathoracic co-injection of $4 \times 10^7$ PFU of Ad-*GFP* and $4 \times 10^7$ PFU of OBP-301. The large tumors were labeled in spots with GFP fluorescence; small nodules, however, could be imaged entirely as intensive GFP signals. Histological analysis confirmed the presence of disseminated tumor cells in the sites of fluorescence emission (Fig. 6). The thoracic cavity of non-tumor-bearing mice was negative for *GFP* transgene expression (data not shown).

## DISCUSSION

Gene-based therapeutic strategies, including replacement of defective tumor suppressors, enhancement of immune-mediated tumor surveillance, and tumor-selective virotherapy, have emerged as promising adjuvants to conventional modalities for human cancer (18-21). We previously reported the development of a tumor-specific replication-selective adenovirus, OBP-301 or "Telomelysin", which is capable of exclusively replicating in telomerase-positive human cancer cells (12). In the current study, we investigated the potential of OBP-301 to visualize human tumors by facilitating replication of a GFP-expressing replication-deficient adenovirus, Ad-*GFP*. As reported previously (8), for real-time imaging of growing tumors in live mice, GFP appears to be an extremely effective tumor cell marker to identify tumor tissues at a single-cell level. A major advantage of GFP labeling is that imaging requires no preparative procedures such as contrast agents, substrates, and light-tight boxes as do other imaging techniques.

Elevated levels of telomerase activity are found in the majority of malignancies (Fig. 1A) and are believed to play a critical role in tumorigenesis (22). Therefore, telomerase-specific OBP-301 was able to selectively compensate the E1 gene products for Ad-*GFP* that lacks E1 proteins in human tumor cells, but not in normal cells. However, as the recombinant adenovirus vectors can efficiently infect a wide variety of dividing and nondividing cells, and transfer exogenous genes into mammalian cells, Ad-*GFP* infection alone at high concentrations may induce GFP fluorescence non-selectively in both tumor and normal cells. Our preliminary experiments

demonstrated that Ad-*GFP* infection alone at less than 1.0 MOI was insufficient to induce GFP expression under fluorescence microscopy in most tumor and normal cells *in vitro* (data not shown). We confirmed that co-infection of 0.1 MOI of Ad-GFP and 1.0 MOI of OBP-301 could express GFP fluorescence selectively in tumor cells, although detectable green signals were evident with Ad-*GFP* infection alone in cells sensitive to adenovirus infection, such as H1299 cells (Fig. 2). However, the fact that most normal cells are relatively resistant to adenovirus infection suggests that the false-positive detection of normal cells is likely to be less frequent.

It has been reported that $1.6 \times 10^9$ PFU of Ad-*GFP* delivered to various organs induced high intensity GFP expression that could be visualized by whole-body imaging (11) and, therefore, we determined $10^7$ PFU of Ad-*GFP* as a suboptimal dose for GFP detection *in vivo* by the dose titration study (Fig. 3). Indeed, intratumoral injection of $8 \times 10^5$ PFU of Ad-*GFP* plus $8 \times 10^6$ PFU of OBP-301 resulted in intensive GFP expression in tumors, whereas no GFP signals were detectable by subcutaneous administration of these vectors into normal areas (Figs. 4 and 5). CCD imaging demonstrated the heterogeneous pattern of GFP expression only in tumors in mice that received intratumoral injection of 50 μl of the vector solution, suggesting that the vectors might not be able to spread throughout the tumor tissues (Fig. 5). Moreover, the green signals in tumors disappeared within 14 days after intratumoral injection of Ad-*GFP* and OBP-301, presumably by the dilution of vectors with tumor cell proliferation (Fig. 5). We previously showed that intratumoral injection of OBP-301 was effective for suppressing the growth of H1299 human lung tumors subcutaneously transplanted into *nu/nu* mice (12); $8 \times 10^6$ PFU of OBP-301, however, might be

insufficient for growth inhibition of SW620 and A549 tumors. Further studies are required to determine optimal doses of the vectors to obtain complete and prolonged GFP labeling of solid tumors.

Progression of non-small cell lung cancer is characterized by the dissemination of malignant pulmonary epithelial cells (23). To overcome the poor prognosis of lung cancer involving the pleura, innovative methodology for early diagnosis as well as treatment is needed. We previously reported that intrathoracic injection of replication-deficient adenovirus expressing antisense against heparanase, which is associated with metastatic potential, inhibited pleural dissemination of human lung cancer cells in an orthotopic murine model (17). These observations suggest that intrathoracic administration of adenovirus is capable of infecting disseminated neoplastic nodules in the thoracic cavity. Obstacles to effective diagnosis and therapy for pleural dissemination include the fact that tumors that are either too small or hidden in an internal body location could not be visually detected. Our optical CCD imaging was able to visualize tiny foci of pleural dissemination of A549 human lung cancer cells with GFP fluorescence after intrathoracic injection of OBP-301 and Ad-*GFP*, although these lesions could not be macroscopically identified (Fig. 6). Several studies have demonstrated the utility of CCD imaging to track metastasis and/or dissemination of tumor cells that were stably transfected with the *GFP* gene in small animals (6-10); the vector-based strategy in the present study, however, is considered more convenient and clinically relevant. If target lesions can be identified during thoracotomy, surgeons are capable of removing disseminated tumors. Moreover, a future option may be to develop robotic laser therapy for pleural dissemination with an automatic detection tool that

chases GFP fluorescence under thoracoscopy.

The approach is considered to be promising; it also; however, suffers from some limitations. For example, tumors existing within organs could not be detected, as it requires exposing the tumors to a Xenon lamp. Because the entire tumors were not fluorescent except very tiny tumors, the margins of invasive tumors that are not clearly encapsulated might go unseen. In addition, the distant metastatic tumors could not be visualized by intratumorally or regionally injected OBP-301 and Ad-*GFP*. As a means to circumvent this limitation, the development of the tumor-specific replication-selective adenovirus (OBP-401), in which the *GFP* gene was inserted, has allowed systemic administration, leading to the whole-body distribution of the vector, thereby detecting distant metastatic lesions with telomerase-specific GFP expression. Preclinical studies using OBP-401 are currently underway in our laboratory.

In conclusion, our data presented here indicate that locoregional injection of Ad-*GFP* plus OBP-301 in combination with highly sensitive CCD imaging might be a useful diagnostic strategy for real-time visualization of macroscopically invisible tumor tissues. Although the sensitivity and specificity of the method must be assessed by further experiments, this technology provides a foundation for future clinical application.

## REFERENCES

1) Tearney GJ, Brezinski ME, Bouma BE, Boppart SA, Pitris C, Southern JF, and Fujimoto JG. *In vivo* endoscopic optical biopsy with optical coherence tomography. *Science*, 276: 2037-2039, 1997.

2) MacDonald SL, and Hansell DM. Staging of non-small cell lung cancer: imaging of intrathoracic disease. *Eur. J. Radiol.*, 45: 18-30, 2003.

3) Misteli T, and Spector DL. Applications of the green fluorescent protein in cell biology and biotechnology. *Nat. Biotechnol.*, 15: 961-964, 1997.

4) van Roessel P, and Brand AH. Imaging into the future: visualizing gene expression and protein interactions with fluorescent proteins. *Nat. Cell. Biol.*, 4: E15-20, 2002.

5) Ehrhardt D. GFP technology for live cell imaging. *Curr. Opin. Plant. Biol.*, 6: 622-628, 2003.

6) Rashidi B, Yang M, Jiang P, Baranov E, An Z, Wang X, Moossa AR, and Hoffman RM. A highly metastatic Lewis lung carcinoma orthotopic green fluorescent protein model. *Clin. Exp. Metastasis*, 18: 57-60, 2000.

7) Yang M, Baranov E, Jiang P, Sun FX, Li XM, Li L, Hasegawa S, Bouvet M, Al-Tuwaijri M, Chishima T, Shimada H, Moossa AR, Penman S, and Hoffman RM. Whole-body optical imaging of green fluorescent protein-expressing tumors and metastases. *Proc. Natl. Acad. Sci. USA*, 97: 1206-1211, 2000.

8) Hoffman RM. Visualization of GFP-expressing tumors and metastasis *in vivo*. *Biotechniques* 30: 1016-1022, 1024-1026, 2001.

9) Bouvet M, Wang J, Nardin SR, Nassirpour R, Yang M, Baranov E, Jiang P, Moossa AR, and Hoffman RM. Real-time optical imaging of primary tumor growth and multiple metastatic events in a pancreatic cancer orthotopic model. *Cancer Res.*, 62: 1534-1540, 2002.

10) Yamamoto N, Yang M, Jiang P, Tsuchiya H, Tomita K, Moossa AR, and Hoffman RM. Real-time GFP imaging of spontaneous HT-1080 fibrosarcoma lung metastases. *Clin. Exp. Metastasis*, 20: 181-185, 2003.

11) Yang M, Baranov E, Moossa AR, Penman S, and Hoffman RM. Visualizing gene expression by whole-body fluorescence imaging. *Proc. Natl. Acad. Sci. USA*, 97: 12278-12282, 2000.

12) Kawashima T, Kagawa S, Kobayashi N, Shirakiya Y, Umeoka T, Teraishi F, Taki M, Kyo S, Tanaka N, and Fujiwara T. Telomerase-specific

replication-selective virotherapy for human cancer. *Clin. Cancer Res.*, 10: 285-292, 2004.

13) Kim NW, Piatyszek MA, Prowse KR, Harley CB, West MD, Ho PL, Coviello GM, Wright WE, Weinrich SL, and Shay JW. Specific association of human telomerase activity with immortal cells and cancer. *Science*, 266: 2011-2015, 1994.

14) Shay JW, and Wright WE. Telomerase activity in human cancer. *Curr. Opin. Oncol.*, 8: 66-71, 1996.

15) Shay JW, and Wright WE. Telomerase: a target for cancer therapeutics. *Cancer Cell*, 2: 257-265, 2002.

16) Nakayama J, Tahara H, Tahara E, Saito M, Ito K, Nakamura H, Nakanishi T, Tahara E, Ide T, and Ishikawa F. Telomerase activation by hTRT in human normal fibroblasts and hepatocellular carcinomas. *Nat. Genet.*, 18: 65-68, 1998.

17) Uno F, Fujiwara T, Takata Y, Ohtani S, Katsuda K, Takaoka M, Ohkawa T, Naomoto Y, Nakajima M, and Tanaka N. Antisense-mediated suppression of human heparanase gene expression inhibits pleural dissemination of human cancer cells. *Cancer Res.*, 61: 7855-7860, 2001.

18) Shao J, Fujiwara T, Kadowaki Y, Fukazawa T, Waku T, Itoshima T, Yamatsuji T, Nishizaki M, Roth JA, and Tanaka N. Overexpression of the wild-type p53 gene inhibits NF-kB activity and synergizes with aspirin to induce apoptosis in human colon cancer cells. *Oncogene*, 19: 726-736, 2000.

19) Waku T, Fujiwara T, Shao J, Itoshima T, Murakami T, Kataoka M, Gomi S, Roth JA, and Tanaka N. Contribution of CD95 ligand-induced neutrophil infiltration to the bystander effect in p53 gene therapy for human cancer. *J. Immunol.*, 165: 5884-5890, 2000.

20) Itoshima T, Fujiwara T, Waku T, Shao J, Kataoka M, Yarbrough WG, Liu TJ, Roth JA, Tanaka N, and Kodama M. Induction of apoptosis in human esophageal cancer cells by sequential transfer of the wild-type p53 and E2F-1 genes: involvement of p53 accumulation via ARF-mediated MDM2 down-regulation. *Clin. Cancer Res.*, 6: 2851-2859, 2000.

21) Ohtani S, Kagawa S, Tango Y, Umeoka T, Tokunaga N, Tsunemitsu Y, Roth JA, Taya Y, Tanaka N, and Fujiwara T. Quantitative analysis of p53-targeted gene expression and visualization of p53 transcriptional activity following intratumoral administration of adenoviral p53 *in vivo*. *Mol. Cancer Ther.*, 3: 93-100, 2004.

22) Masutomi K, and Hahn WC. Telomerase and tumorigenesis. *Cancer Lett.*, 194:

163-172, 2003.

23) Fukuse T, Hirata T, Tanaka F, and Wada H. The prognostic significance of malignant pleural effusion at the time of thoracotomy in patients with non-small cell lung cancer. *Lung Cancer*, 34: 75-81, 2001.

## Figure Legends

**Fig. 1** **(A)** Relative *hTERT* mRNA expression in human tumor and normal cells determined by real-time RT-PCR analysis. The *hTERT* mRNA expression of A549 human lung cancer cells was considered as 1.0 and the relative expression level of each cell line was calculated against that of A549 cells. **(B)** Schematic DNA structures of OBP-301 and Ad-*GFP*. OBP-301 contains the hTERT promoter sequence inserted into the E3-deleted adenovirus genome to drive transcription of the E1A and E1B bicistronic cassette linked by the IRES structure. The Ad-*GFP* vector contains the GFP cDNA driven by the CMV promoter.

**Fig. 2** Selective bystander replication of Ad-*GFP* in the presence of OBP-301 in human cancer cells *in vitro*. Cultured human cancer (SW620 [colorectal], A549 [lung], and H1299 [lung]) and normal cells (WI-38, NHLF, and HUVEC) were infected with 0.1 MOI of Ad-*GFP* alone or in combination with 1.0 MOI of OBP-301, and photographed under the fluorescent microscope for GFP expression 24 hours after treatments. $\times$ 200 magnification.

**Fig. 3** External images of non-tumor-bearing *nu/nu* mice injected with increasing doses of Ad-*GFP* alone. Non-tumor-bearing mice were subcutaneously injected with $1.3 \times 10^6$, $1.3 \times 10^7$, $1.3 \times 10^8$, or $1.3 \times 10^9$ PFU of Ad-*GFP* alone and documented as photographs for GFP expression by the CCD non-invasive imaging system 24 hours after injection.

**Fig. 4** **(A)** External images of non-tumor-bearing mice injected with Ad-*GFP* plus OBP-301. As a control, non-tumor-bearing mice received subcutaneous injection with $8 \times 10^5$ PFU of Ad-*GFP* in combination with $8 \times 10^6$ PFU of OBP-301, and then were assessed for GFP fluorescence 24 hours after administration. As expected, no GFP signals were obtained. *Left upper panel*: macroscopic appearance of mouse. **(B)** External images of SW620 tumor-bearing *nu/nu* mice injected with Ad-*GFP* alone. Three weeks after subcutaneous inoculation of SW620 tumor cells ($5 \times 10^6$ cells/mouse), mice received intratumoral injection of Ad-*GFP* at the density of $8 \times 10^5$ PFU alone. As expected, no GFP fluorescence expression was detected for at least 7 days post-injection. *Left panels*: macroscopic appearance of SW620 tumors; *right panels:* fluorescent detection.

**Fig. 5** Time course of external images of subcutaneous SW620 and A549 tumors after intratumoral injection of Ad-*GFP* plus OBP-301. Three weeks after subcutaneous inoculation of SW620 and A549 tumor cells ($5 \times 10^6$ cells/mouse), Ad-*GFP* and OBP-301 at the concentrations of $8 \times 10^5$ PFU and $8 \times 10^6$ PFU, respectively, were directly injected into established tumors. The GFP fluorescence intensity was monitored for 7 consecutive days under the CCD non-invasive imaging system. *Left panels*: macroscopic appearance of subcutaneous tumors; *right panels:* fluorescent detection.

**Fig. 6** Internal images of pleural dissemination visualized by intrathoracic

injection of Ad-*GFP* and OBP-301. Female BALB/c *nu*/*nu* mice were intrathoracically implanted with 5 x $10^6$ A549 tumor cells. Two weeks later, $4 \times 10^7$ PFU/50 μl each of Ad-*GFP* and OBP-301 were injected into the thoracic space. Five days after virus injection, mice were sacrificed and their thoracic spaces were examined. Three representative mice are shown. *Left panel:* fluorescent detection; *right panel:* gross appearance of A549 tumors grown orthotopically in the thoracic spaces. *Arrows*, disseminated tiny tumor. Left lower panel: hematoxylin-eosin staining of the lesion of fluorescence emission. × 100 magnification.

Fig. 1A

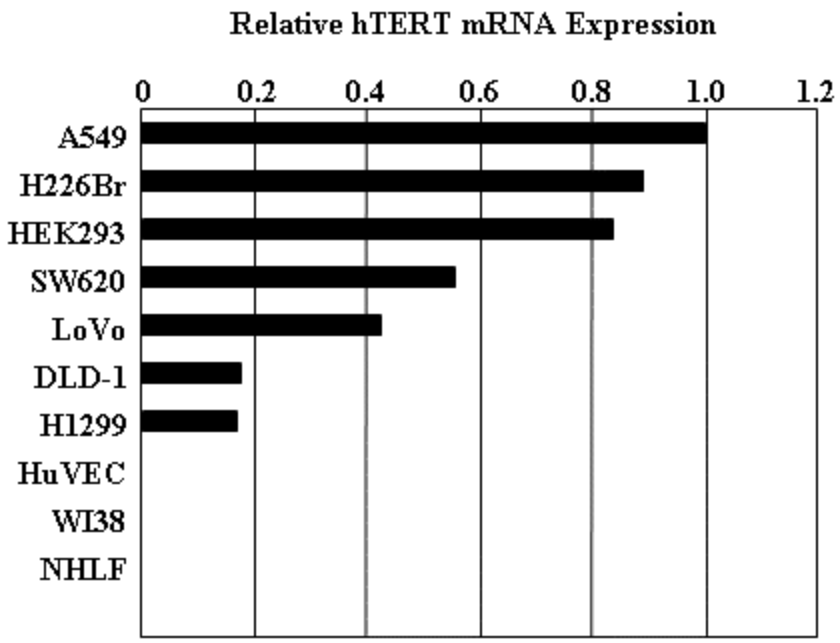
Relative hTERT mRNA Expression
0
0.2
0.4
0.6
0.8
1.0
1.2
A549
H226Br
HEK293
SW620
LoVo
DLD-1
H1299
HuVEC
WI38
NHLF

Fig. 1B

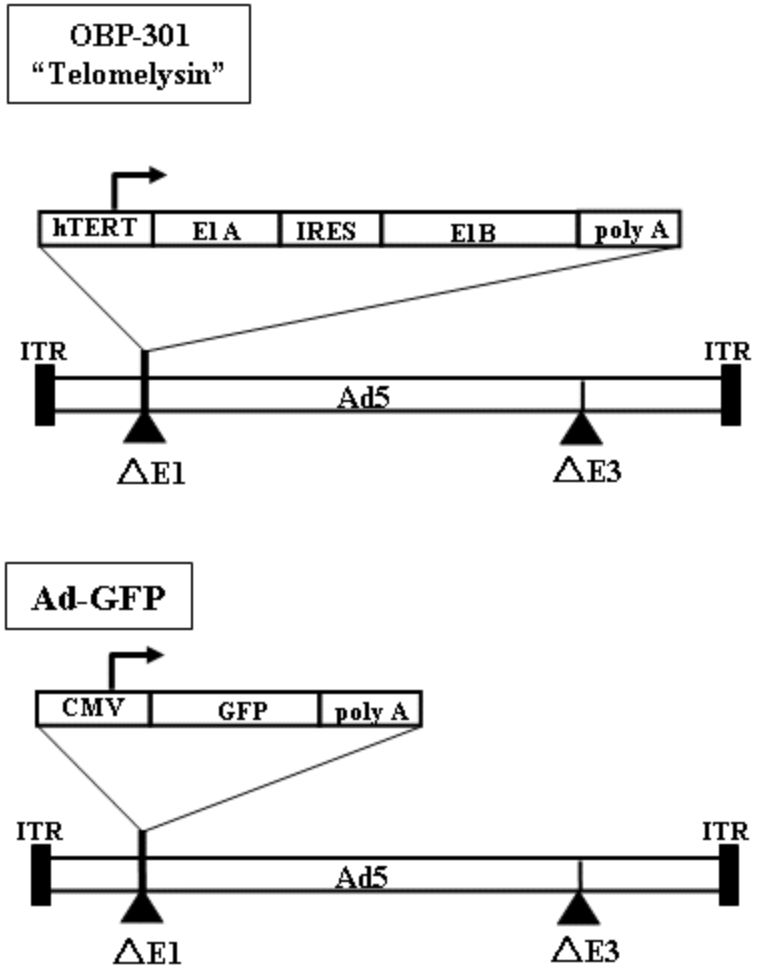
OBP-301
"Telomelysin"
hTERT
E1A
IRES
E1B
poly A
ITR
ITR
Ad5
ΔE1
ΔE3
Ad-GFP
CMV
GFP
poly A
ITR
ITR
Ad5
ΔE1
ΔE3

Fig. 2

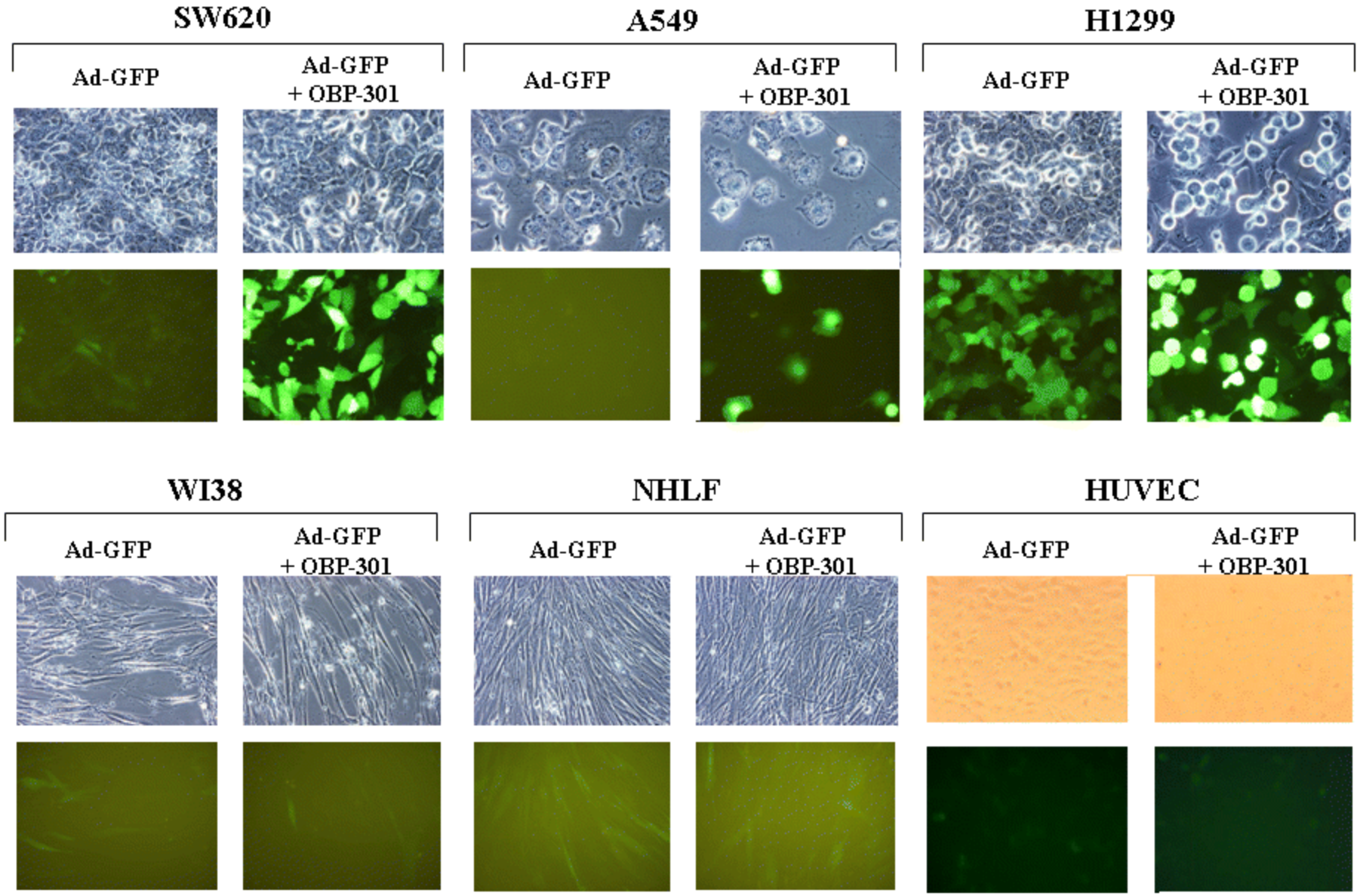
SW620
Ad-GFP
Ad-GFP + OBP-301
A549
Ad-GFP
Ad-GFP + OBP-301
H1299
Ad-GFP
Ad-GFP + OBP-301
WI38
Ad-GFP
Ad-GFP + OBP-301
NHLF
Ad-GFP
Ad-GFP + OBP-301
HUVEC
Ad-GFP
Ad-GFP + OBP-301

Fig. 3

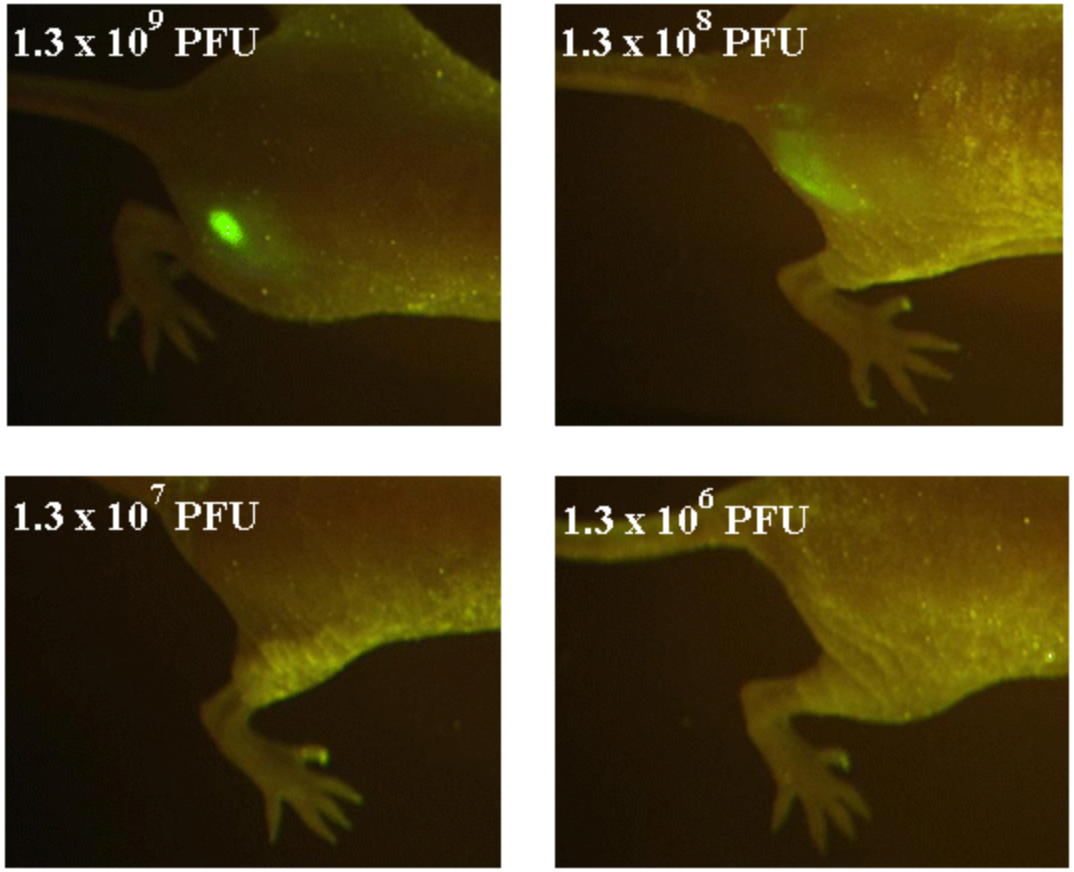

Fig. 4

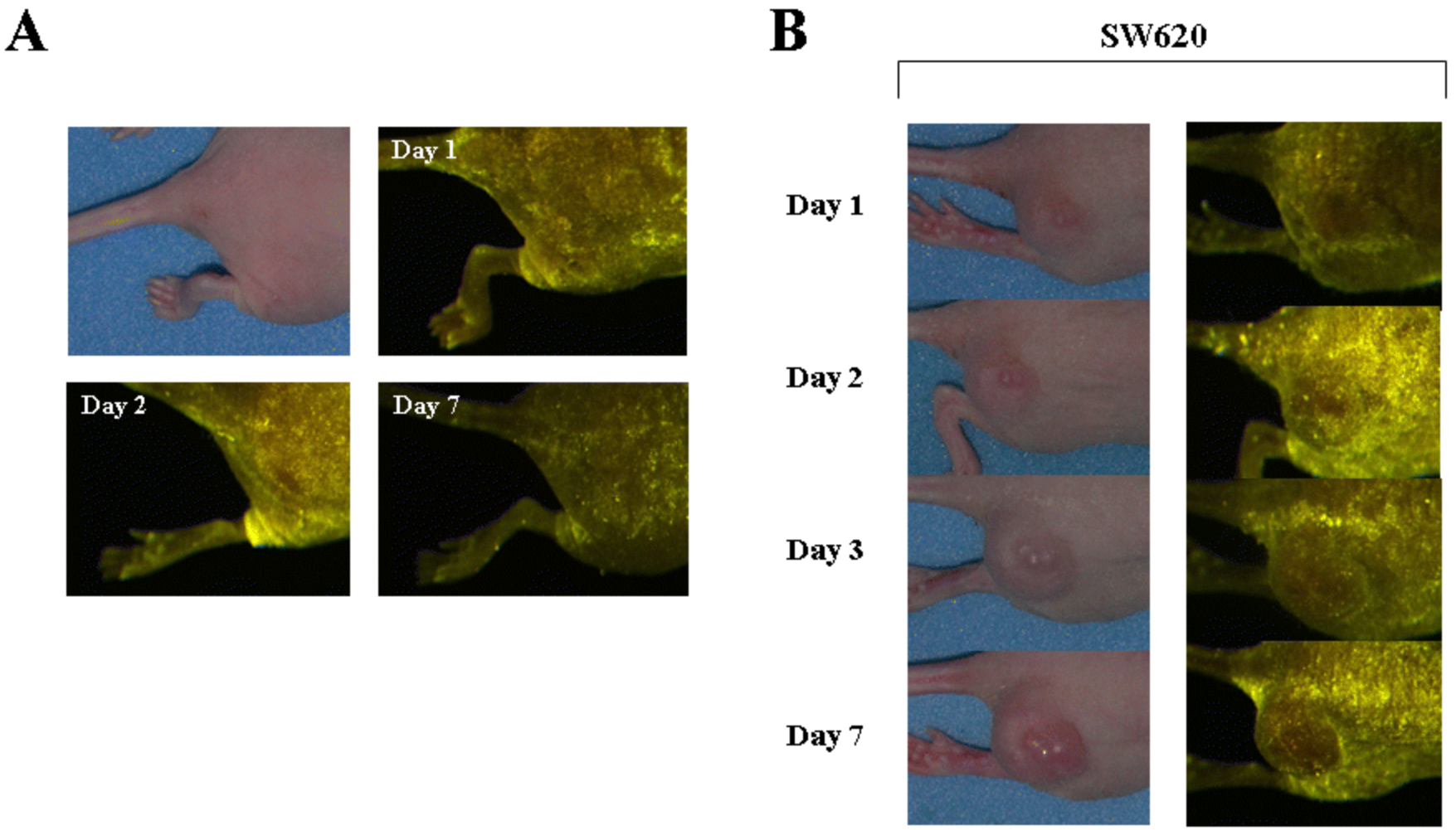

Fig. 5

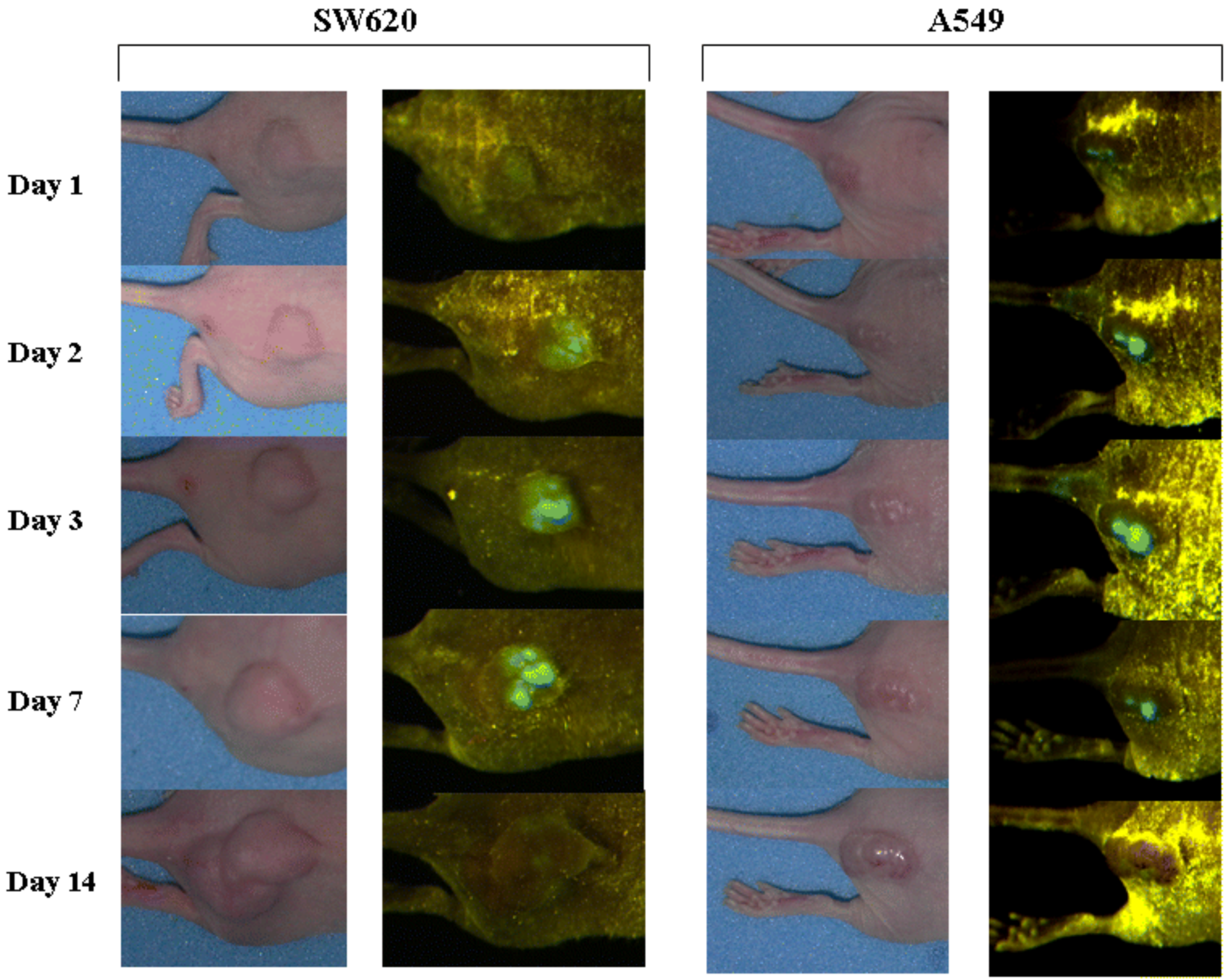

Fig. 6